Article

Experimental and Theoretical Charge Density Study of Chemical Bonding in a Co Dimer Complex

Jacob Overgaard, Henrik F. Clausen, Jamie A. Platts, and Bo B. Iversen

J. Am. Chem. Soc., **2008**, 130 (12), 3834-3843• DOI: 10.1021/ja076152c • Publication Date (Web): 04 March 2008

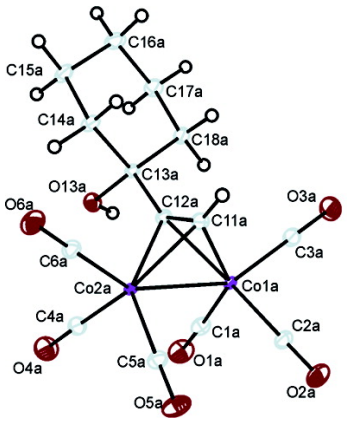

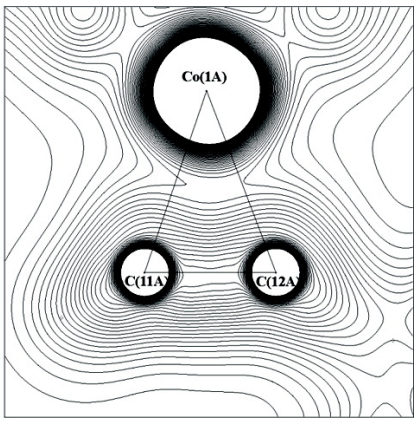

More About This Article

Additional resources and features associated with this article are available within the HTML version:

- Supporting Information
- Links to the 2 articles that cite this article, as of the time of this article download
- Access to high resolution figures
- Links to articles and content related to this article
- Copyright permission to reproduce figures and/or text from this article

View the Full Text HTML

J|A|C|S
ARTICLES
Published on Web 03/04/2008

Experimental and Theoretical Charge Density Study of Chemical Bonding in a Co Dimer Complex

Jacob Overgaard,*,† Henrik F. Clausen,† Jamie A. Platts,‡ and Bo B. Iversen†

Department of Chemistry and the Interdisciplinary Nanoscience Center, University of Aarhus, Langelandsgade 140, 8000 Aarhus C, Denmark, and School of Chemistry, Cardiff University, Park Place, Cardiff CF10 3AT, U.K.

Received August 20, 2007; E-mail: jacobo@chem.au.dk

Abstract: The charge density of $Co_2(CO)_6(HC{\equiv}CC_6H_{10}OH)$ (**1**) in the crystalline state has been determined using multipolar refinement of single-crystal X-ray diffraction data collected (i) with a synchrotron source at very low temperatures (15 K) and (ii) using a conventional source with the crystal at intermediate temperature (100 K). The X-ray charge density model is augmented by complete active space and density functional theory calculations. Topological analyses of the different charge distributions show that the two Co atoms are not bonded to each other in the quantum theory of atoms in molecules (QTAIM) sense of the word. However, the behavior of the source function and the total energy density indicate that there is some bond-like character in the Co−Co interaction. The bridging alkyne fragment provides an unusual bonding situation, with extremely small electron density differences between the two Co−C bond critical points and the "CoC_2" ring critical point. Thus, the structure is close to a topological catastrophe point. Comparison of the results obtained from the two diffraction data sets and *ab initio* theory suggests that the topology of the experimental electron density in this special atomic environment is highly sensitive to subtle effects of measurement errors and potential shortcomings of the multipole model, or to effects of the crystal field. Thus, even the two identical molecules in the asymmetric unit show altered bonding patterns.

Introduction

The nature of the chemical bonding in metal dimers and clusters has been the subject of increased interest in recent years.[1] A number of methods, experimental as well as theoretical, have been introduced in attempts to analyze the bonding situation in such compounds. The archetypal models attracting the most attention are metal−carbonyl dimers, such as $Co_2(CO)_8$, which can bond with or without bridging carbonyl groups. Closely related to these compounds are alkyne-bridged dicobalt complexes, composed of $Co(CO)_3$ dimers bridged by an alkyne, which find use in organic synthesis via the Pauson−Khand reaction, a method for regioselective synthesis of cyclopentanones,[2] and in nanotechnology as models for electronic communication along molecular wires.[3] Cobalt−alkyne complexes also show interesting anti-tumor properties and hold promise for use in treatments for leukemia, although the mode of this action has not been identified.[4]

Conventional electron counting suggests that these compounds should exhibit a Co−Co single bond, in line with magnetic measurements showing them to have a singlet ground state and the fact that no line-broadening is seen in NMR spectra. However, recent theoretical analysis of a model compound shows a more complex situation:[5] a more appropriate designation is of a singlet diradical; i.e., the electronic structure has partial occupation of Co−Co bonding and antibonding orbitals. This finds support in topological analysis of the electron density, which does not present any bonding interaction in the form of a bond critical point (bcp)[6] between the two Co atoms. On the other hand, it has been suggested[7] that a topological analysis of the total electron density is insufficient for location of bonding interactions in metal dimers, but analysis of the total energy density and other descriptors can provide powerful insight into bonding patterns where conventional electron density analysis proves problematic.[8] This has been illustrated for $Co_2(CO)_7$, where energy density analysis gives evidence of a stabilizing metal−metal interaction not found using the electron density alone.[7]

More recently, Gatti has developed a novel method of analysis based on the source function[9] that allows identification of the origin of electron densities and bonding interactions, and which

† University of Aarhus.
‡ Cardiff University.

(1) (a) Leung, P.; Coppens, P. *Acta Crystallogr., Sect. B* **1983**, *39*, 535. (b) Bianchi, R.; Gervasio, G.; Marabello, D. *Acta Crystallogr., Sect. B* **2001**, *57*, 638−645. (c) Bianchi, R.; Gervasio, G.; Marabello, D. *Helv. Chim. Acta* **2001**, *84*, 722−734. (d) Bianchi, R.; Gervasio, G.; Marabello, D. *Chem. Commun.* **1998**, 1535−1536. (e) Bianchi, R.; Gervasio, G.; Marabello, D. *Inorg. Chem.* **2000**, *39*, 2360−2366. (f) Macchi, P.; Proserpio, D. M.; Sironi, A. *J. Am. Chem. Soc.* **1998**, *120*, 13429−13435. (g) Macchi, P.; Garlaschelli, L.; Martinengo, S.; Sironi, A. *J. Am. Chem. Soc.* **1999**, *121*, 10428−10429. (h) Farrugia, L. J.; Mallinson, P. R.; Stewart, B. *Acta Crystallogr., Sect. B* **2003**, *59*, 234−247.
(2) See, for example: Geis, O.; Schmalz, H.-G. *Angew. Chem., Int. Ed.* **1998**, *37*, 911.
(3) Low, P. J.; Rousseau, R.; Lam, P.; Udachin, K. A.; Enright, G. D.; Tse, J. S.; Wayner, D. D. M.; Carty, A. J. *Organometallics* **1999**, *18*, 3885.
(4) Ott, I.; Kircher, B.; Gust, R. *J. Inorg. Biochem.* **2004**, *98*, 485−489.
(5) Platts, J. A.; Evans, G. J. S.; Coogan, M. P.; Overgaard, J. *Inorg. Chem.* **2007**, *46*, 6291−6298.
(6) Bader, R. F. W. *Atoms in Molecules: A Quantum Theory*; Clarendon Press: Oxford, U.K. 1990.
(7) Finger, M.; Reinhold, J. *Inorg. Chem.* **2003**, *42*, 8128−8130.
(8) (a) Cremer, D.; Kraka, E. *Angew. Chem., Int. Ed. Engl.* **1984**, *23*, 627. (b) Cremer, D.; Kraka, E. *Croat. Chem. Acta* **1984**, *57*, 1259.
(9) Bader, R. F. W.; Gatti, C. *Chem. Phys. Lett.* **1998**, *287*, 233−238.

10.1021/ja076152c CCC: $40.75

has previously been successfully applied to hydrogen bonding[10] as well as to the study of metal−metal bonds.[11] Gatti et al.[11] conclude that previously successful descriptors of the nature of bonding, such as the sign of the Laplacian or evaluation of the ratio V/G and to some extent also the total energy density, H, at the bcp's, fail in the classification of these particular bonding types for metal−metal bonds. However, theoretical delocalization indices based on the atomic overlap matrix, and related definitions of bond order, do demonstrate trends that can be used to describe these interactions.[12] The source function to some extent mimics the behavior of these indices, and it is therefore a very useful, experimentally derivable property which may be used in the categorization of metal−metal bonding.

There are thus numerous methods available for the analysis of bonding in metal dimer complexes. The present study employs a combination of these methods, originating from both experimental and theoretical data, on $Co_2(CO)_6(HC{\equiv}CC_6H_{10}OH)$ (**1**), in which the bridging alkyne bears one hydrogen and one cyclohexanol group. This compound makes a useful comparison to previous work on similar compounds[5] and is also in itself an interesting test case, as it crystallizes with two molecules in the asymmetric unit ($Z' = 2$). This allows comparison of the electron density in identical molecules using a single data set. Furthermore, the alkyne bridge presents an unusual bonding situation that poses substantial challenges to theoretical as well as experimental methods. To substantiate our conclusions, we present data from two independent single-crystal X-ray diffraction experiments using different X-ray sources and different data collection temperatures.

Experimental Section

Conventional Data Collection. A dark-red single crystal of **1**, synthesized according to published procedures,[13] with dimensions of $0.30 \times 0.40 \times 0.59$ mm^3, was attached with oil to a goniometer head and mounted on a Mo Kα-radiation-equipped Bruker X8 Apex2 diffractometer at the University of Aarhus. The crystal temperature was adjusted to 100(1) K using an Oxford Cryosystems CryostreamPlus 700 liquid nitrogen device. The orientation matrix was initially determined from a small set of frames and used in the program COSMO[14] to plan a data collection strategy with full completeness to a resolution of 1.1 Å^{-1} and maximum redundancy. Compound **1** is found to crystallize in the centrosymmetric triclinic space group $P\bar{1}$, with two independent molecules in the asymmetric unit. Twenty-one sets of data were collected, and these were subsequently integrated using SAINT+[15] to give a total of 155 851 reflections with a maximum resolution of 1.189 Å^{-1}. The data were corrected for absorption using multiple measurements in SORTAV,[16] with resultant minimum and maximum transmission factors of 0.442 and 0.575. The intensities were averaged with SORTAV[17] to 40 271 unique reflections with an average redundancy of 3.9 and $R_{int} = 3.4\%$. For the refinements, reflections measured only once were omitted, and the final *hkl* file included 29 382 intensities.

The structure was solved using the direct methods program SHELXS.[18] This found all non-hydrogen atoms, and subsequently all hydrogens were inserted in calculated positions in a riding model refinement. The independent atom model (IAM) refinements were performed with SHELXL-97.[18] A complete IAM model consists of 422 parameters, and the refinement converges smoothly to $R_w(F^2) = 8.1\%$, $R_{F>4\sigma(F)}(F) = 3.1\%$, with significant residuals around the Co atoms. Extinction was found to be significant and was refined with an empirical model in SHELXL to a maximum correction of around 4%.

The charge density distribution was modeled using the program XD,[19] based on the multipole formalism suggested by Hansen and Coppens.[20] The IAM model was used as a starting point for these refinements. Prior to refinements, all hydrogen atoms were translated along their bond axis such that the bond lengths correspond to tabulated average values from neutron studies.[21] The thermal parameters for hydrogen were fixed during refinements at 150% of the equivalent isotropic thermal parameter of their parent atom. All atomic scattering factors were taken from the neutral atoms, with f' and f'' calculated with the program FPRIME.[22] Initially, a high-angle refinement including reflections above 0.8 Å^{-1} provided an estimate of the positional and thermal parameters, which were then subsequently held fixed during the initial refinement of the multipole parameters. The final model included hexadecapoles on the Co atoms, octupoles on the C and O atoms, and only a bond-directed dipole and a monopole on the hydrogen atoms. The H atoms were divided into three groups, and within each group a common set of multipole parameters were used. The groups consists of the alkyne-H, the hydroxyl-H, and finally the remaining methylene-H's.

The radial behavior of the multipoles can be changed by refinement of κ parameters. These are initially common to all atoms of the same type; however, greater flexibility of the model can be achieved by discriminating among, for instance, alkyne-C, methylene-C, and carbonyl-C. We used six different sets of κ parameters where, for each atom type, κ'' was kept identical for all values of l (the refined values are deposited in the Supporting Information, Table S7). Extinction was refined, and the maximum correction was 6.0% for reflection (021). The extinction type was mosaic spread Lorentzian type 1.[23] Only a few experimental charge density studies have been carried out on $Z' > 1$ crystals,[24] and while it doubles the number of parameters, it also affords a possibility to study the transferability of multipole parameters within the same data, and hence without differences in systematic errors. On the other hand, the internal comparison can also be used to impose constraints, helping the refinement to reach the global minimum. In this study, no chemical constraints were imposed to make the two molecules identical, and the final model thus consists of 785 parameters, which resulted in $R(F^2) = 2.34\%$ and a goodness-of-fit (GoF) of 1.29. Convergence of a joint refinement of positional, thermal, and multipolar parameters with 1199 parameters is unproblematic, however, with a slight decrease in the quality of the rigid bond test and only marginal

(10) Overgaard, J.; Schiøtt, B.; Larsen, F. K.; Iversen, B. B. *Chem. Eur. J.* **2001**, *7*, 3756−3767. Gatti, C.; Bertini, L. *Acta Crystallogr. Sect. A* **2004**, *60*, 438−449. Gatti, C.; Cargnoni, F.; Bertini, L. *J. Comput. Chem.* **2003**, *24*, 422−436.
(11) Gatti, C.; Lasi, D. *Faraday Discuss.* **2007**, *135*, 55.
(12) Macchi, P.; Sironi, A. *Coord. Chem. Rev.* **2003**, *238*−*239*, 383−412
(13) Greenfield, H.; Sternberg, H. W.; Friedel, R. A.; Wotiz, J. H.; Markby, R.; Wender, I. *J. Am. Chem. Soc.* **1956**, *78*, 120−124.
(14) *COSMO*, Data collection strategy program; Bruker AXS Inc.: Madison, WI.
(15) *SAINT*, v7.12A; Bruker AXS Inc.: Madison, WI, 2005.
(16) Blessing, R. H. *Acta Crystallogr., Sect. A* **1995**, *51*, 33−38.
(17) Blessing, R. H. *J. Appl. Crystallogr.* **1997**, *30*, 421−426. Blessing, R. H. *Crystallogr. Rev.* **1989**, *1*, 3−58.
(18) Sheldrick, G. M. *SHELX-97*, Programs for Crystal Structure Analysis, Release 97-2; Institüt für Anorganische Chemie der Universität Göttingen: Göttingen, Germany, 1998.
(19) Volkov, A.; Macchi, P.; Farrugia, L. J.; Gatti, C.; Mallinson, P.; Richter, T.; Koritsanszky, T. *XD2006*, A Computer Program Package for Multipole Refinement, Topological Analysis of Charge Densities and Evaluation of Intermolecular Energies from Experimental and Theoretical Structure Factors; 2006.
(20) Hansen, N. K.; Coppens, P. *Acta Crystallogr., Sect. A* **1979**, *39*, 909−921.
(21) Allen, F. H.; Kennard, O.; Watson, D. G.; Brammer, L.; Orpen, A. G.; Taylor, R. J. *J. Chem. Soc., Perkin Trans. 2* **1987**, 1−19.
(22) Cromer, D. L. *Acta Crystallogr.* **1965**, *18*, 17−23.
(23) Becker, P. J.; Coppens, P. *Acta Crystallogr., Sect. A* **1974**, *30*, 129−147.
(24) Milanesio, M.; Bianchi, R.; Ugliengo, P.; Roetti, C.; Viterbo, D. *J. Mol. Struct.: THEOCHEM* **1997**, *419*, 139−154. Pichon-Pesme, V.; Lecomte, C. *Acta Crystallogr., Sect. B* **1998**, *54*, 485−493. Hambley, T. W.; Hibbs, D. E.; Turner, P.; Howard, S. T.; Hursthouse, M. B. *J. Chem. Soc., Perkin Trans. 2* **2002**, *2*, 235−239. Overgaard, J.; Schiøtt, B.; Larsen, F. K.; Iversen, B. B. *Chem. Eur. J.* **2001**, *7*, 3756−3767. Overgaard, J.; Waller, M. P.; Platts, J. A.; Hibbs, D. E. *J. Phys. Chem. A* **2003**, *107*, 11201−11208. Rodel, E.; Messerschmidt, M.; Dittrich, B.; Luger, P. *Org. Biol. Chem.* **2006**, *4*, 475−481. May, E.; Destro, R.; Gatti, C. *J. Am. Chem. Soc.* **2001**, *123*, 12248.

Table 1. Crystallographic Details and Refinement Statistics for **1**

	conventional	synchrotron
formula	$Co_2(CO)_6(HC_2C_6H_{11}O)$	$Co_2(CO)_6(HC_2C_6H_{11}O)$
formula weight, g mol^{-1}	820.19	820.19
crystal size, mm	0.30 × 0.40 × 0.59	0.17 × 0.20 × 0.23
crystal system	triclinic	triclinic
space group	$P\bar{1}$	$P\bar{1}$
λ, Å	0.71073	0.47686
T, K	100	15
a, Å	9.3125(3)	9.2850(3)
b, Å	10.3768(3)	10.3240(3)
c, Å	17.4885(6)	17.4010(6)
α, °	73.477(1)	73.611(1)
β, °	78.215(2)	78.185(2)
γ, °	83.078(1)	82.979(1)
V, Å^3	1582.5(1)	1562.7(1)
F(000)	824.0	824.0
ρ, g cm^{-3}	1.721	1.743
μ, mm^{-1}	2.13	0.66
T_{max}, T_{min}	0.575, 0.442	0.971, 0.940
$\sin(\theta)/\lambda_{max}$, Å	1.189	1.112
N_{meas}, $N_{discarded}$	160 908, 5 057	390 837, 11 295
N_{unique}	40 270	31 948
average redundancy	3.9	11.9
completeness	0.90	0.89
h,k,l ranges	−21 to 21; −23 to 24; 0 to 41	−19 to 20; −21to 22; 0 to 38
R_{int}	0.034	0.056
N_{obs}, N_{var}; ($F^2 > 2\sigma(F^2)$)[a]	23 438, 785	28 940, 1 228
$R_w(F)$, $R_w(F^2)$; $F^2 > 2\sigma(F^2)$	0.018, 0.035	0.018, 0.036
weighting scheme	$1/\sigma(F^2)^2$	$1/\sigma(F^2)^2$
$R(F)$, $R(F^2)$; all data	0.045, 0.026	0.019, 0.024
goodness-of-fit	1.29	1.78

[a] The difference in the number of parameters reflects that the synchrotron model used joint refinement of positional, thermal, and multipole parameters.

improvement in residual. A simple comparison of 406 common multipole parameters from molecules A and B gave an average difference of 0.042 with an rmsd of 0.044, suggesting that the multipole refinement is well-converged and that the electron density is similar across the two independent molecules. The maximum and minimum residuals are found near the Co atoms at values of 0.33 e Å^{-3} (1.05 Å from Co(1A)) and −0.28 e Å^{-3} (0.42 Å from C(3A)). The Hirshfeld rigid bond test[25] was satisfied, with a largest difference of mean-square displacement amplitudes of 0.0011 Å^2 for C(1A)−O(1A). The average value for the 30 bonds was 0.0004 Å^2. Full crystallographic details are available in Table 1, while an ORTEP drawing[26] is shown in Figure 1.

Synchrotron Data Collection. A dark-red crystal with side lengths of 0.17, 0.20, and 0.23 mm was mounted on the Huber four-circle diffractometer installed at beamline D3 at Hasylab, Hamburg. The crystal was kept at a constant temperature of 15(2) K using a liquid He Helijet setup. The beamline is equipped with a Mar165 CCD detector that was kept fixed at a 2θ angle of −15° during the entire data collection, which lasted 14.5 h. In that time, six series of data comprising 1489 frames were collected using φ-rotations of 1°. The exposure time was either 4 or 40 s, and the wavelength was 0.47686 Å. The completeness of the data was optimized by changing the value of χ within the physical limitations afforded in the small hutch environment.

The resulting data were integrated using the program XDS,[27] and a local program[28] that corrects for oblique incidence into the detector was used to prepare files for absorption correction and averaging by the program SORTAV.[16] An empirical absorption correction gave minimum and maximum transmission factors of 0.940 and 0.971, respectively. The 379 542 collected reflections were averaged to 31 948 unique reflections with an average redundancy of 11.9 and an internal agreement of 5.6%. However, the average values hide a large increase in R_{int} for the weak high-order data, which for the outermost shells reaches 25% (see Supporting Information). The 589 singly and doubly observed reflections were discarded, as were 1051 reflections exhibiting excessively large deviations from calculated values based on an independent atom model ($|\Delta F|/\sigma(F) > 10$). The latter reflections appeared on the detector surface in regions partly shadowed by the cooling equipment.

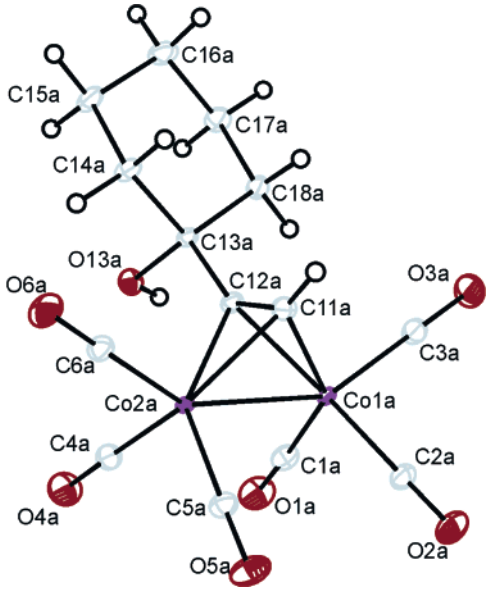

Figure 1. ORTEP drawing of the A molecule of **1** based on the synchrotron data. The thermal ellipsoids for non-hydrogen atoms are shown at the 90% probability level.

The structural model from the conventional data (see above) was adopted and refined against the synchrotron data. This leads to $R_w(F^2)$ = 6.9%, $R_{F>4\sigma(F)}$ = 2.5%, and also for this crystal extinction is

(25) Hirshfeld, F. L. *Acta Crystallogr.* **1976**, *A32*, 239−244.
(26) Farrugia, L. J. *J. Appl. Crystallogr.* **1997**, *30*, 565.
(27) Kabsch, W. *J. Appl. Crystallogr.* **1993**, *26*, 795−800.
(28) Overgaard, J.; Madsen, G. K. H. Program D3_red to reduce data collected at the D3 beamline at Hasylab, available from the authors on request.

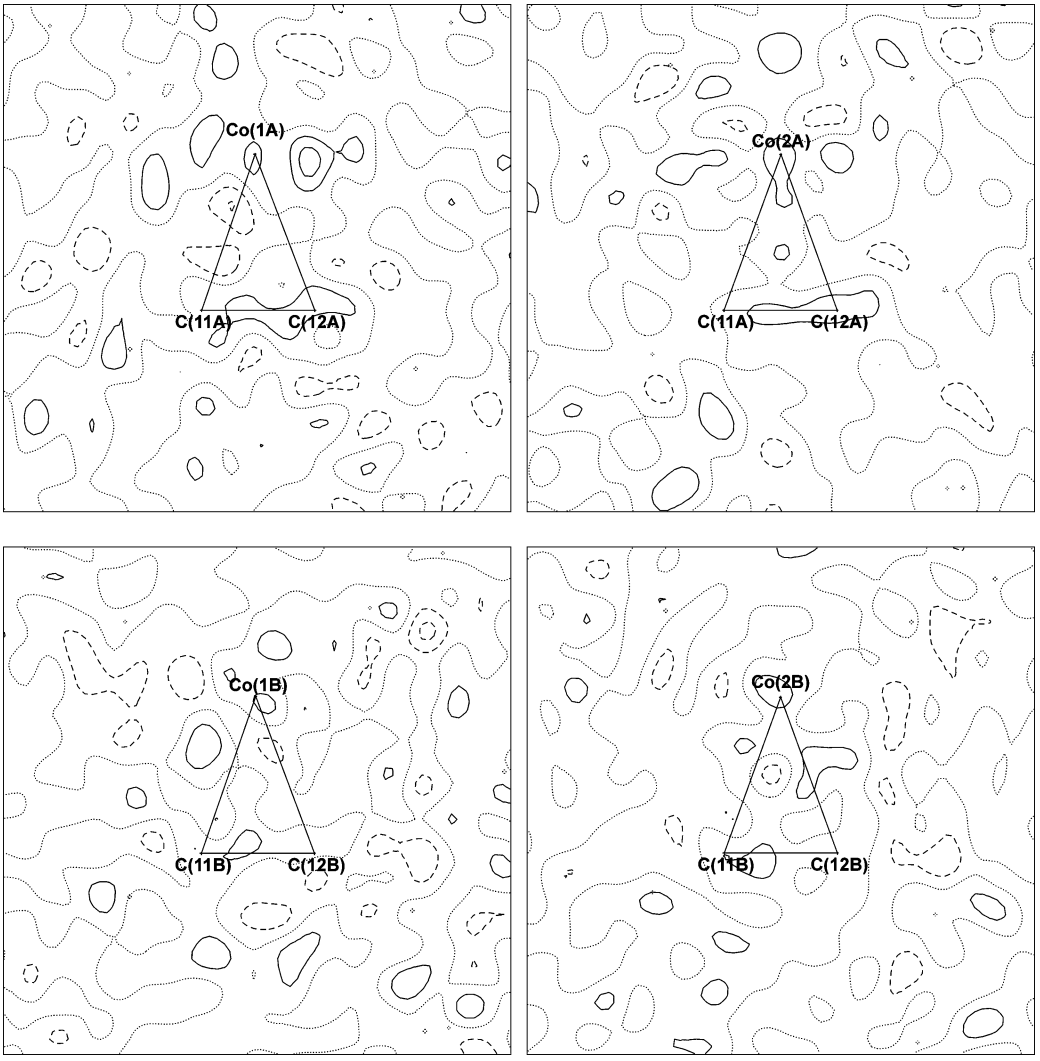

Figure 2. Residual density in the four Co−C_2(alkyne) planes. The contour intervals are 0.1 e Å^{-3}; positive contours are shown with solid lines, negative contours with dashes, and the zero contour with dots. The resolution is 0.9 Å^{-1} (see text for details).

significant, with the maximum correction being 2.2% for reflection (023). The maximum extinction-corrected reflection in the conventional experiment, (021), was blocked in the synchrotron experiment and thus not included in the data. This IAM model was imported into XD,[19] and a procedure analogous to the conventional data refinement was followed to reach an essentially identical multipole model. The final residuals are $R_{all}(F^2) = 2.4\%$ and GoF = 1.8. The minimum and maximum residuals are in the vicinity of the Co atoms, with values around ±0.5 e Å^{-3} when all data are used in the Fourier summation. Limiting the summation to reflections having values of $\sin(\theta)/\lambda$ below 0.9 Å^{-1} reduces residual values to less than ±0.25 e Å^{-3} (Figure 2). Unsuccessful tests were performed to further reduce the residuals around Co: third- and fourth-order Gram−Charlier coefficients were insignificant, and allowing the values of κ'' to vary with l also had no effect. The large increase in residual density observed when including the high-order data prompted us to examine these reflections in more detail. The merging of equivalent reflections shows clearly that the internal agreement increases steeply at higher scattering angle (Supporting Information, Figure S5), concurrently with a decrease in redundancy compared with the low-order data. Thus, the weak reflections contribute disproportionately to the residual density while not carrying much information about the electronic model. We therefore decided to remove those reflections with deviations of more than 3 s.u.'s from the final multipole model as well as those with ratios of I_o/I_c higher than 3.0 or smaller than 0.333. This reduced the total number of unique reflections by 11.4%, with an expected significant reduction in residuals ($R_{all}(F^2)$ now 1.9%). The residual density maps in the four Co−C_2 planes after this procedure are shown in the Supporting Information (Figure S7). As expected, this has no influence on the multipole model: the average change in the 70 monopole values is 0.02(5), while the average change for all multipoles is 0.01(2). Also, the thermal parameters are unchanged, with an average absolute change in U_{ij} of 0.0005(19), showing that the weak outlier reflections contribute noise but little additional information. Further details of this analysis can be found in the Supporting Information.

The rigid-bond test was performed on the final model, showing fine correspondence between thermal parameters: an average difference of mean-square ADPs for bonds not involving H or Co of 0.0003 Å^2 is excellent.[25]

The source function calculations on the experimental models were carried out using the XDPROP module of XD with the keywords SOURCE and TOPINT.

Theoretical Calculations. Following previous work on a smaller, symmetrical model compound,[5] complete active space self-consistent field (CAS-SCF) calculations were carried out to examine the electron density in **1**. Cartesian coordinates of one molecule from the asymmetric unit were extracted, and a restricted Hartree−Fock wavefunction was obtained, using a basis set consisting of 6-31G(f) on Co[29] and Dunning's cc-pVDZ on C, O, and H.[30] On Co, f-type polarization functions were taken from the work of Ehlers et al.[31] The stability of the RHF

Table 2. Selected Bond Distances Involving the Co Atoms of **1**

	conventional		synchrotron	
bond	A	B	A	B
Co(1)−Co(2)	2.46482(13)	2.46660(14)	2.46334(9)	2.46534(8)
Co(1)−C(11)	1.9544(5)	1.9669(5)	1.9551(3)	1.9679(3)
Co(1)−C(12)	1.9797(5)	1.9857(5)	1.9807(3)	1.9856(3)
Co(2)−C(11)	1.9669(5)	1.9620(5)	1.9657(3)	1.9629(3)
Co(2)−C(12)	1.9663(5)	1.9685(5)	1.9630(3)	1.9642(3)
Co(1)−C(1)	1.8069(7)	1.8172(6)	1.8039(3)	1.8170(3)
Co(1)−C(2)	1.8363(6)	1.8343(6)	1.8363(3)	1.8342(3)
Co(1)−C(3)	1.8003(7)	1.7954(7)	1.8005(4)	1.7931(3)
Co(2)−C(4)	1.8316(6)	1.8240(6)	1.8316(3)	1.8282(3)
Co(2)−C(5)	1.8191(6)	1.8192(6)	1.8195(3)	1.8195(3)
Co(2)−C(6)	1.7911(5)	1.8031(7)	1.7910(3)	1.8036(3)
C(11)−C(12)	1.3433(7)	1.3401(6)	1.3421(4)	1.3399(4)

wavefunction was tested using the criteria of Seeger and Pople,[32] yielding a UHF singlet solution. The natural orbitals from this were used as the input for CAS-SCF calculations, with all orbitals involving Co 3d functions along with π and π^* included in the active space, leading to 22 electrons in 14 orbitals, denoted CAS[22,14]. In addition, density functional theory (DFT) calculations were carried out using the BLYP functional with the same basis set, a method that was shown to reproduce *ab initio* spectroscopic and density properties in a model compound.[5] All theoretical electron density data were produced using the AIMPAC[33] and AIM2000[34] programs, while the local source was calculated with a modified version of the PROAIMV code.[35]

Results and Discussion

The present study forms part of a process of evaluating the diffraction data from the recently modified synchrotron beamline D3 at Hasylab, which has a particular emphasis on charge density studies. Technical details of the beamline setup and data reduction will be published elsewhere,[36] while here we report on data as well as model comparison, in addition to interpretation of the derived electron density. There are a number of criteria that can be used to assess the quality of the two data sets. The simple statistics of the fitting procedure, such as *R*-factors (Table 1), give the first indication that both data sets are of excellent quality. Slightly smaller *R*-factors are observed with the synchrotron data; however, the goodness-of-fit of the conventional data is closer to unity, and both data sets are complete to a relatively high scattering angle. A plot of the ratio of observed to calculated intensities based on the final model is given in the Supporting Information (Figure S6), which shows a larger spread in the conventional data. The geometries of the structural models (selected details in Table 2) are very similar, with the largest deviation between conventional and synchrotron models of just 0.2% and an average difference of 0.06% between bond lengths in the two models. It is thus not in the normal structural parameters that the differences in the data are manifested,

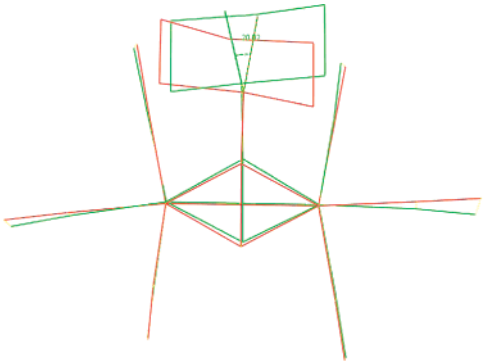

Figure 3. Structure overlay prepared by Mercury[37] of the two independent molecules of **1**. The hydrogen atoms are omitted for clarity. The overlay is calculated on the basis of all non-H atoms excluding the atoms in the cyclohexanol. This gives a rms distance of 0.13 Å for the 17 distances.

although standard deviations on these parameters are noticeably smaller from the synchrotron data than from the conventional source.

The crystal structure of **1** exhibits two highly similar independent molecules, with the only real difference being in the orientation of the cyclohexanol moeity, which differs by a rotation around an axis through the C(12)−C(13) bond of ca. 20°. This is illustrated in Figure 3, which shows a structural overlay of the two molecules. It should be noted that the two Co(1)−C(alkyne) bonds are different by about 0.02 Å, while the difference is an order of magnitude smaller for the Co(2)−C(alkyne) bonds. It is hard to find an explanation for this in the crystal structure, as a noncrystallographic mirror plane containing the alkyne and bisecting the Co(1)−Co(2) line implies that the chemical environments of the Co atoms are very similar. It is also worth noting the distribution of bond lengths for the three Co−C(CO) bonds for each Co atom. For Co(1A), there are two very similar short Co−C bonds (1.80 Å) and one long bond (1.83 Å), while the other three Co atoms have one short, one long, and also one intermediate bond (1.82 Å), a feature evident in both synchrotron and conventional data. The Co−Co internuclear distance in **1** of 2.465 Å is similar to those in other compounds of the same type.[38]

The systematic errors are unquestionably smaller in the synchrotron data than in the conventional data, as the former is based on an experiment carried out with significantly shorter wavelength, at a lower temperature and with a smaller crystal, and therefore the effects of absorption, thermal diffuse scattering, and extinction are reduced.[39] Despite this, extremely similar molecular geometries are obtained from the two methods, and in general similar electron density properties are also obtained. One approach to quantifying the similarity of the two data sets is to use the density properties at all bcp's, a method termed "quantum topological molecular similarity" by Popelier.[40] This approach indicates quite different densities from the two data sets with an average deviation of 3.5, or 0.8 without using the data from the carbonyl C−O bonds. For comparison, Popelier

(29) (a) Windus, T. L. *J. Chem. Phys.* **1998**, *109*, 1223. (b) Wachters, A. J. H. *J. Chem. Phys.* **1970**, *52*, 1033. (c) Hay, P. J. *J. Chem. Phys.* **1977**, *66*, 4377.
(30) Dunning, T. H., Jr. *J. Chem. Phys.* **1989**, *90*, 1007.
(31) Ehlers, A. W.; Bohme, M.; Dapprich, S.; Gobbi, A.; Hijllwarth, A.; Jonas, V.; Kohler, K. F.; Stegmann, R.; Veldkamp, A.; Frenking, G. *Chem. Phys. Lett.* **1993**, *208*, 111.
(32) Seeger, R.; Pople, J. A. *J. Chem. Phys.* **1977**, *66*, 3045.
(33) Biegler-König, F. W.; Bader, R. F. W.; Tang, T.-H. *J. Comput. Chem.* **1982**, *3*, 317 (these programs can be obtained from http://www.chemistry.mcmaster.ca/aimpac).
(34) Biegler-König, F. W.; Schönbohm, J. *J. Comput. Chem.* **2002**, *23*, 1489.
(35) Program PROAIM, modified by Prof. Carlo Gatti to enable the calculation of the source function.
(36) Poulsen, R. D.; Jørgensen, M. R. V.; Overgaard, J.; Larsen, F. K.; Morgenroth, W.; Graber, T.; Chen, Y.-S.; Iversen, B. B. *Chem. Eur. J.* **2007**, *13*, 9775−9790.
(37) Macrae, C. F.; Edgington, P. R.; McCabe, P.; Pidcock, E.; Shields, G. P.; Taylor, R.; Towler, M.; van de Streek, J. *J. Appl. Crystallogr.* **2006**, *39*, 453−457.
(38) Gregson, D.; Howard, J. A. K. *Acta Crystallogr., Sect. C* **1983**, *39*, 1024−1027.
(39) Larsen, F. K. *Acta Crystallogr., Sect. B* **1995**, *51*, 468−482. Iversen, B. B.; Larsen, F. K.; Pinkerton, A. A.; Martin, A.; Darovsky, A.; Reynolds, P. A. *Acta Crystallogr., Sect. B* **1999**, *55*, 363−374.
(40) Popelier, P. L. A. *J. Phys. Chem. A* **1999**, *103*, 2883−2890. O'Brien, S. E.; Popelier, P. L. A. *J. Chem. Inf. Comput. Sci.* **2001**, *41*, 764−775.

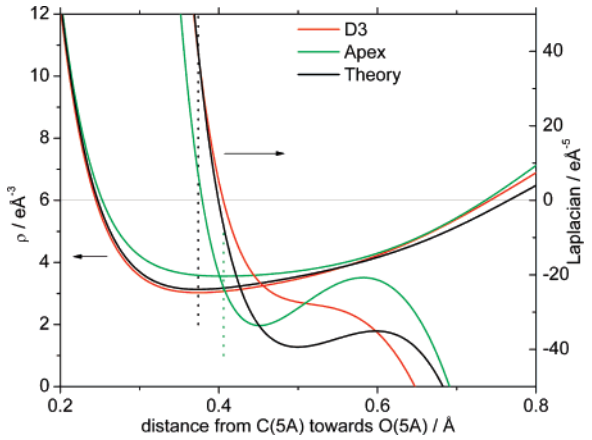

Figure 4. Behavior of ρ and $\nabla^2\rho$ along the C−O bond. Vertical lines indicate the position of the bcp (bcp's from theory and D3 are at the same position), while the horizontal arrows show which curves are depicting ρ and $\nabla^2\rho$, respectively. It should be noted that the lines from theory are using BLYP values, as the CAS-SCF approach does not include C−O orbitals in the active space.

reports a value of 0.37 between *p*-NH_2 and *p*-NO_2 benzoic acid. This slightly surprising result appears to be due to the characteristics of the density in the carbonyl bonds, as illustrated in Figure 4. The values of $\nabla^2\rho_c$ from the conventional data and the synchrotron data have different signs at the bcp, negative for the former and positive for the latter, leading to very large variations between the data sets for these bonds. Much of this difference stems from a small shift in the position of the bcp, which is *ca.* 0.03 Å closer to C in the synchrotron data, which in a region of quickly varying $\nabla^2\rho$ causes large changes.[41,42] For comparison, ρ and $\nabla^2\rho$ values from DFT are included in Figure 4. There is excellent agreement between the total density curves of the synchrotron data and theory, but even here the Laplacian shows significant discrepancies, especially in the region closer to oxygen (to the right of Figure 4). Close to the bcp, however, the two curves are much closer, leading to similar values of $\nabla^2\rho_c$ for synchrotron and theory. The obvious fundamental difference between the two experimental descriptions of these polar C−O bonds, i.e., different signs of the Laplacian at the bcp, is a reminder that, for such bond types, the evaluation of topological properties at a single point only (the bcp) is not sufficient to categorize the bonding nature, and a more systematic analysis of the entire density distribution is required.

Apart from this feature of the C−O bonds, overall there is much similarity between the electron densities obtained from synchrotron and conventional data; however, when compared with theory, there are indications (e.g., Figure 4) that the former represents the better model. It should be noted that certain integrated properties are found (for instance, the Co atomic charges, see below) for which the conventional model resembles the theoretical density better; however, similarly, a number of other properties give the opposite result. In the better established regions away from the uncertain Co−C bonds, the synchrotron data provide the better model. Therefore all experimental data analysis reported in the following will, unless indicated, be based on the synchrotron model. Furthermore, analysis of the conventional model leads to similar conclusions, and most illustrations and tables presented for the synchrotron model are, for the sake of completeness, given for the conventional data in the Supporting Information.

A topological analysis of the total experimental electron density was performed in order to investigate the nature of the chemical bonding in **1**, and the results, with particular emphasis on the bonding of the Co atoms, are shown in Table 3 (complete tables are given in the Supporting Information). The first, most obvious result that can be observed in Table 3 is that, in molecule A, only two Co−C_{alkyne} bcp's are located, while in molecule B, four such interactions are present. In this regard, the data for molecule B compare well with the CAS-SCF results, which also locate four Co−C_{alkyne} bcp's, in correspondence with previous theoretical work. This difference prompted us to look more closely at the properties of these bonds. The small values of λ_2 in the Co−C(alkyne) bonds is noteworthy. This signifies that the density in a direction perpendicular to the interatomic line is rather flat, hence leading to problems identifying the position of the bcp's. Another conspicuous, related feature is the lengths of the Co−C bond paths compared to the interatomic distances, which are also shown in Table 3. In the experimental model, the bond paths are as much as 0.12 Å (or 6%) longer than the geometrical bond lengths. For comparison, Table 3 also shows results for the Co−C(CO) and C−O bonds, which illustrate the more typical behavior of these conventional bonds, including the similarity of bond path and internuclear lengths and the larger value of λ_2.

To examine the origins of these unusual density properties, the electron densities in the four different CoC_2 regions are illustrated below (Figure 5). The bcp is located approximately at the midpoint of the Co−C interatomic line, and it is immediately clear that, in this central region, the density varies very slowly in the direction perpendicular to the Co−C "bonds". The density decreases quickly outside the CoC_2 triangles, but when moving beyond the bond toward the center of the triangle, the density does not noticeably decrease. Instead, a plateau seems to have been reached without any significant decrease in the center. This plateau can be more clearly seen in Figure 6, which plots the electron density along lines from the ring centroid, through the bcp's (if present, otherwise the Co−C midpoint) and beyond to the exterior of the CoC_2 triangles. These plots show very small increases in density from the ring center to the bcp, in the range 0.01−0.03 e $Å^{-3}$. The theoretical data supports that the density is very flat within these triangles, although increases in density from ring to bond are slightly larger (0.02−0.05 e $Å^{-3}$).

This bonding situation is of particular interest, since the density is extremely flat, and hence only a slight change in the density would make the Co−C bcp coalesce with the ring critical point (rcp). Such a change would lead to the emergence of a T-shaped structure, termed a catastrophe point in nuclear configuration space.[6] When the bcp and rcp coalesce, the molecular graph is fundamentally changed, and catastrophe points are often associated with unstable structures. Here, the phenomenon is observed in the crystalline state, but it is absent in the isolated molecule. This may indicate that crystal field effects induce sufficient changes in the electron density to alter

(41) Birkedal, H.; Madsen, D.; Mathiesen, R. H.; Knudsen, K.; Weber, H.-P.; Pattison, P.; Schwarzenbach, D. *Acta Crystallogr., Sect. A* **2004**, *60*, 371−381.

(42) It is surprising to find the bcp closer to the C atom in the C−O bonds in the synchrotron model, as the κ-value for C is substantially lower and thus the atom more expanded than is the case for the conventional model (Table S7, Supporting Information).

Table 3. Topological Analysis of the Electron Densities[a]

bond	$\rho_c(r)$	$\nabla^2\rho_c(r)$	d_{1-2}	d_{1-bcp}	L_{bp}	λ_1	λ_2	λ_3
Co(1)−C(11)	N/A[b]	N/A[b]	N/A[b]	N/A[b]	N/A[b]	N/A[b]	N/A[b]	N/A[b]
	0.766(5)	8.3(1)	1.968	0.989	2.047	−3.10	−0.45	11.85
	0.753	5.8	1.954	0.977	1.961	−3.01	−1.86	10.71
Co(1)−C(12)	0.713(5)	8.0(1)	1.981	0.996	2.097	−3.07	−0.94	11.97
	0.765(5)	7.8(1)	2.019	1.002	2.123	−3.20	−0.47	11.48
	0.724	5.7	1.980	0.987	1.987	−2.81	−1.39	9.89
Co(2)−C(11)	N/A[b]	N/A[b]	N/A[b]	N/A[b]	N/A[b]	N/A[b]	N/A[b]	N/A[b]
	0.703(5)	8.8(1)	1.963	0.990	2.064	−2.45	−0.42	11.70
	0.736	6.0	1.968	0.982	1.975	−2.92	−1.56	10.45
Co(2)−C(12)	0.755(5)	8.1(1)	1.963	0.986	2.042	−3.20	−1.22	12.52
	0.704(6)	7.8(10)	1.964	0.993	2.038	−2.74	−1.21	11.73
	0.742	5.7	1.966	0.980	1.975	−2.95	−1.68	10.36
Co−C average	0.95(3)	12.8(12)	1.81(2)	0.90(1)	1.82(2)	−4.4(3)	−3.6(4)	21(1)
	0.93(6)	12.8(8)	1.82(2)	0.90(1)	1.82(1)	−4.2(3)	−3.5(6)	21(1)
	0.88(3)	17.1(8)	1.81(2)	0.89(1)	1.82(2)	−3.3(2)	−2.9(10)	23(1)
C(11)−C(12)	2.240(13)	−21.8(1)	1.345	0.697	1.347	−12.67	−11.50	2.34
	2.200(13)	−20.2(1)	1.344	0.697	1.346	−11.79	−10.99	2.58
	2.199	−19.0	1.343	0.617	1.351	−13.78	−12.58	7.38
C−O average	3.13(6)	24(8)	1.141(3)	0.763(3)	N/A	−35(1)	−34(1)	92(8)
	3.13(8)	23(8)	1.139(2)	0.762(2)	N/A	−35(1)	−33(1)	92(8)
	3.18(2)	36(1)	1.139(3)	0.767(2)	N/A	−38.9(3)	−38.7(4)	113(2)

[a] For each bond, the first two lines are experimental results for molecules A and B, and the third line gives the theoretical results. The table lists the values of the electron density at the bcp (ρ_c, e Å^{-3}), the Laplacian at the bcp ($\nabla^2\rho_c$, e Å^{-5}), the internuclear distance (d_{1-2}, Å), the distance from atom 1 to the bcp (d_{1-bcp}, Å), and the length of the bond path (L_{bp}, Å). The eigenvalues of the diagonalized Hessian matrix, λ_i, are given in units of e Å^{-5}. [b] No critical point located.

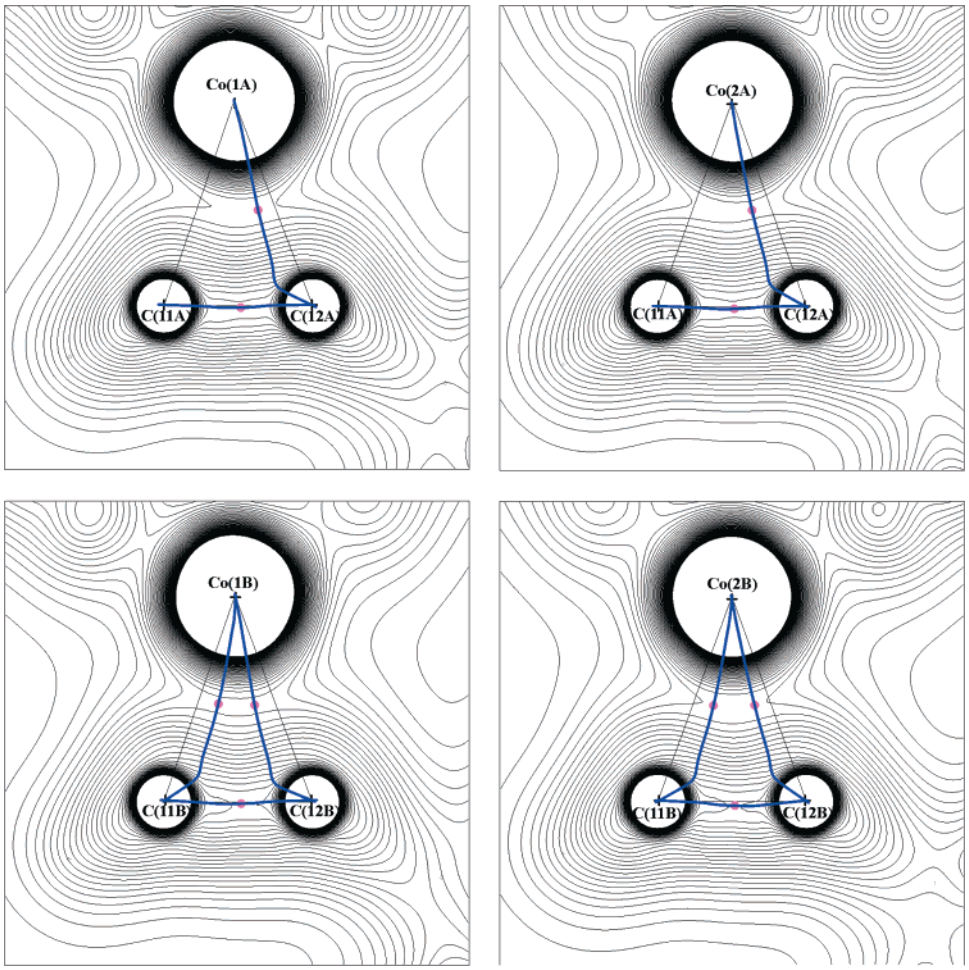

Figure 5. Density in the four Co−C−C planes of the molecule. The maps show also the molecular graph with blue lines, with bcp's indicated as filled gray circles. The ring critical points in the two lower figures are between the two Co−C bcp's (not shown). The contour intervals are 0.1 e Å^{-3}.

the topology. A theoretical calculation on the periodic crystalline system would test this hypothesis, but that is beyond the scope of the present paper. The asymmetric substitution of the alkyne group may also play a role in this feature of the density, since both "missing" Co−C bonds are to C(11), which bears the hydrogen. However, this seems less likely, as this geometrical

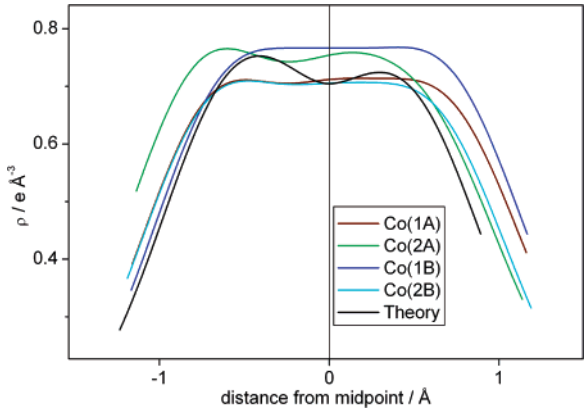

Figure 6. Density along selected paths in the Co−C_2(alkyne) planes from experimental and theoretical values, illustrating the plateau which renders the location of the bcp's very difficult. Negative distances are toward the connection with C(11) (or to the left of the center in Figure 5), while positive is toward C(12).

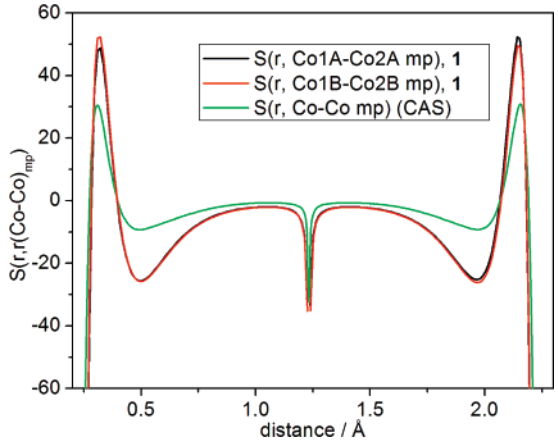

Figure 7. Local source evaluated at the Co−Co midpoint along the Co−Co line. The red and black curves indicate experimental results, while the theoretical results are shown in green.

Table 4. Integrated Source Contributions, *S* (Atom, r_{Co-Co}), to the Density at the Co−Co Midpoint for Molecule A, Listed as Absolute Values and Percentages[a]

atom	S_A, e Å^{-3}	*S* (%)	S_{theo}, e Å^{-3}	*S*(%)
Co(1A)	−0.064	−19.9	0.013	3.9
Co(2A)	−0.058	−18.1	0.014	4.4
C(11A)	0.055	17.1	0.026	8.3
O(1A)	0.049	15.4	0.033	10.3
O(5A)	0.047	14.6	0.034	10.6
C(12A)	0.038	11.9	0.028	8.7
Co(1B)	−0.013	−4.2		
Co(2B)	−0.014	−4.4		

[a] A complete listing for all atoms is given in the Supporting Information. Theoretical data are calculated from the BLYP wavefunction. The fourth and fifth columns give the results from DFT calculations in which only one molecule was included.

asymmetry is also present in molecule B as well as in the theoretical calculations, which nevertheless show the expected topology. Furthermore, the abridged data set (described in the Supporting Information) leads to a clear change of the molecular graph in exactly the region of molecule A where the T-shaped behavior exists, suggesting that the measurement error is the main reason that not all four Co−C(C) bcp's exist.

That measurement errors are the source of the unexpected topology is supported by the residual density in the planes of Figures 5 and 6 (see Figure 2), i.e., the electron density not modeled by the multipole model, which gives an estimate of the error in the measured density. The residuals in these regions have extrema around 0.15 e Å^{-3}, with values of at least 0.1 e Å^{-3} found in all four CoC_2 triangles. The uncertainty that arises from measurement errors and any shortcomings of the multipole model is larger than the theoretically calculated variation in density across the CoC_2 triangles. It is therefore perhaps unsurprising that not all Co−C bcp's can be located, even in a density derived from the high-quality diffraction data used in this case. Overall, it is clear that the present experimental data are of high quality. We argue that the reason for the present failure to correctly locate these particular Co−C(alkyne) bcp's is a combination of measurement errors on the structure factors and/or limitations inherent in the multipole model.[43] For these reasons, the bonding in this type of complexes can be used as a test case for developments in software and hardware. In order to further probe the origins of these problems, we intend to study the effects of adding noise to theoretically calculated structure factors, in a fashion similar to the work of Feil et al.[44]

Having established the problems in describing the CoC_2 regions, we now move to the question of Co−Co bonding. As in previous experimental and theoretical work on related compounds, topological analysis shows no Co−Co bcp: a minimum in ρ is found midway between Co nuclei, but no maximum is observed in the perpendicular direction (see Supporting Information). However, as discussed above, this measure has been criticized as being insufficiently sensitive for proper analysis of metal−metal bonds. Instead, we examine the source function and the energy density in the Co−Co region. Figure 7 shows the local source, LS, evaluated along the Co−Co line, using the midpoint as the reference point, from both experimental and CAS theoretical data. Both plots show striking similarities to the plots reported by Gatti and Lasi for the dicarbonyl bridged isomer of $Co_2(CO)_8$. Those authors showed that such plots can distinguish bonded from nonbonded (in the quantum theory of atoms in molecules, or QTAIM, sense) metal−metal isomers, with a sharp drop in LS close to the midpoint indicative of a lack of bonding interaction. Such a drop is precisely the pattern observed in both the experimental and theoretical data, supporting the finding that a direct Co−Co interaction is not present in **1**.

The local source can be summed over atomic basins to yield the integrated source. Gatti and Lasi argue that the integrated source provides information about the metal−metal bonding, for example, showing that its value increases for the involved metal atoms, eventually to positive values, as the interaction becomes stronger. Table 4 contains integrated experimental source values for selected atoms evaluated at the Co−Co midpoint for molecule A. This reveals substantially negative values for both cobalt atoms, indicating that the metal atoms act as sinks for the density in the intermetallic region. These values are much lower than those reported by Gatti and Lasi for $Co_2(CO)_8$, for which a value of +0.7% is quoted, which on the other hand is more in line with the DFT values also given in Table 4. The present data are therefore in complete accordance with the expectation that the Co−Co bonding is weak

(43) In a recent paper, Farrugia and Evans suggest that random errors in the data may influence the resulting molecular graphs: Farrugia, L. J.; Evans, C. *J. Phys. Chem. A* **2003**, *109*, 8834−8848.
(44) de Vries, R. Y.; Feil, D.; Tsirelson, V. G. *Acta Crystallogr., Sect. B* **2000**, *56*, 118−123.

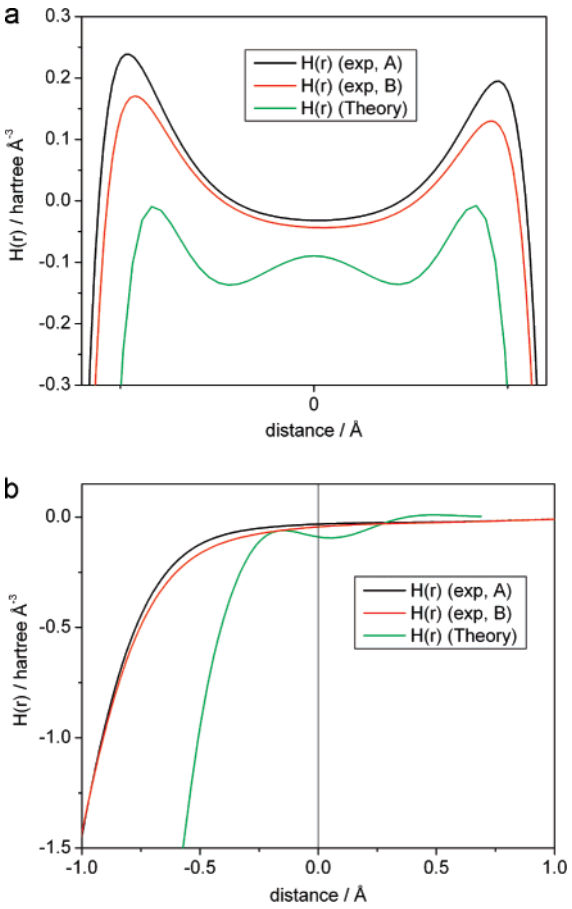

Figure 8. Total energy density, $H(r)$, plotted along (a) the Co−Co line with zero point at the Co−Co midpoint and (b) the C_2 axis that bisects the Co−Co line at the zero point on the x-axis. The units used are hartree Å^{-3} for $H(r)$ and Å for the distance.

in **1**, as ref 11 shows that the integrated source contribution from the metal atoms increases with bond strength.

The behavior of the total energy density, $H(r)$, along two particular lines (one following the Co−Co interaction and one perpendicular to this going through the C−C and the Co−Co midpoints) is shown in Figure 8. Very similar curves are found for molecules A and B, and overall the theoretical plot agrees well with the experimental data, although a slight dip in $H(r)$ is seen in the theoretical plot close to the Co−Co midpoint that is not present in the experimental curve line (Figure 8b). However, the sign of $H(r)$ is negative in the entire range shown, which indicates a stabilizing interaction. This is mimicked along the Co−Co line, where $H(r)$ increases from very negative values to peak at around ±0.5 Å before falling to negative values close to the midpoint (Figure 8a). Again, experimental and theoretical plots are broadly similar but do not agree on some fine details, the theoretical plot showing two minima on either side of the midpoint while the experiment shows one broad minimum at the midpoint.

Further insight into the possible metal−metal bonding may come from the d-orbital populations of the Co atoms, which can be derived from the multipole populations.[45] However, the structure of **1** gives no obvious local coordinate system (LCS) on which to orient the d-orbitals. One possible way of solving this is to choose the LCS that minimizes the orbital cross terms, an idea advanced by Sabino and Coppens and coded into the program ERD.[46] The resulting axes definitions and orbital populations are shown in the Supporting Information (Figure S4 and Table S9, respectively), but these definitions do not convey any useful chemical information. Instead, we have chosen to use an axis convention with the z-axis on Co pointing toward the other Co atom. The d-orbital populations in Table 5 show that the populations of the d(z^2)-orbital are relatively low in all four cases, while for three out of four Co atoms the population of the d(x^2-y^2)-orbital is also low. The former observation is particularly interesting, since it is the bonding/antibonding combinations of d(z^2)-orbitals that give rise to the singlet diradical character determined via UHF and CAS calculations. The observed low populations of these d-orbitals may therefore be related to this electronic structure, although one would also expect lower populations of the d(z^2)- and d(x^2-y^2)-orbitals in the pseudo-octahedral coordination geometry around Co no matter what the Co−Co bonding situation might be.

Table 5. d-orbital Populations[a]

	d(z^2)	d(xz)	d(yz)	d(x^2-y^2)	d(xy)	P_v
Co(1A)	0.985	1.209	1.222	0.946	1.554	5.92
	(16.7)	(20.4)	(20.7)	(16.0)	(26.3)	
Co(1B)	1.146	1.418	1.217	0.878	1.249	5.91
	(19.4)	(24.0)	(20.6)	(14.9)	(21.1)	
Co(2A)	0.847	1.168	1.443	1.301	1.161	5.92
	(14.3)	(19.7)	(24.4)	(22.0)	(19.6)	
Co(2B)	1.073	1.354	1.390	1.063	1.024	5.90
	(18.2)	(22.9)	(23.5)	(18.0)	(17.3)	

[a] The numbers in parentheses give the percentages of the total number of valence electrons on the Co atom carried in the orbital.

Table 6. Atomic Charges and Volumes for Selected Atoms from Integration of the Atomic Basins[a]

atom	$q_X(\Omega)$	$V_{X,001}(\Omega)$	$q_C(\Omega)$	$V_{C,001}(\Omega)$	$q_T(\Omega)$ CAS[6,6]	$V_{T,001}(\Omega)$ CAS[6,6]
Co(1A)	1.506	64.91	0.513	58.97	0.645	70.172
Co(1B)	1.484	65.36	0.497	59.43		
Co(2A)	1.475	64.58	0.433	57.95	0.650	70.339
Co(2B)	1.528	64.46	0.509	58.51		
C(11B)	−0.772	93.26	−0.319	88.38	−0.397	92.123
C(12B)	−0.524	64.23	−0.143	64.56	−0.447	67.015

[a] X refers to the experimental synchrotron model, C to the conventional model, and T to the theoretical density.

Atomic charge and volume data calculated by integration of the relevant atomic basins, Ω, are reported in Table 6 for selected atoms (values for all atoms have been deposited in the Supporting Information, Table S6). First, it is evident from these data that the atomic properties are essentially identical between molecules A and B, where comparison is possible. This is not feasible for C(11A) and C(12A), as integration over atomic basins fails due to the problems in finding the C−Co bcp's discussed above.[47] No charge transfer occurs, and both molecules are observed to be neutral in the synchrotron model, although this is not so for the conventional model, which shows a strange charge transfer of about 0.7 e. Experiment and theory agree on the assignment of a substantial positive charge on each

(45) Holladay, A.; Leung, P.; Coppens, P. *Acta Crystallogr., Sect. A* **1983**, *39*, 377−387.

(46) Sabino, J. R.; Coppens, P. *Acta Crystallogr., Sect. A* **2003**, *59*, 127−131.

(47) If the charges from molecule B are substituted into Table S6A for atoms C(11) and C(12), overall charge neutrality is achieved for both independent molecules, supporting our assertion that atomic properties are transferable across molecules A and B.

Co, but the experimental charge (synchrotron model) is significantly larger. The conventional model gives Co charges in better correspondence with theory, but the atomic volumes, in contrast, agree better between theory and the synchrotron model. Alkyne carbons are negatively charged, and the methods agree on the significant difference in atomic volume between C(11) and C(12). In previous theoretical work, this pattern of charges was also found and was proposed to be a result of back-donation of density from metal-based d-orbitals into the π^*-orbitals of the alkyne. This assignment of bonding modes is supported by the length of the C(11)−C(12) bond, which is closer to the value expected of a C═C double bond than of an alkyne. This is also supported by theoretical bond orders that, in agreement with other recent work, suggest a C−C alkyne bond order of 1.38 (Supporting Information, Figure S12).

Conclusions

We have carried out two accurate diffraction experiments on an alkyne-bridged dicobalt complex, **1**. The first used conditions fairly typical for experimental charge density determinations, i.e., a sealed-tube source of Mo Kα X-rays, a CCD-based area detector, and the crystal held at 100 K. The second employed shorter wavelength X-rays from a synchrotron source, a CCD-based area detector, and liquid helium cooling to 15 K. It is encouraging that the resulting structural and electron density properties of **1** are in close agreement, although the errors in the synchrotron data are smaller than those for the conventional data. The analysis indicates that the recently upgraded synchrotron beamline D3 at Hasylab, which is dedicated to accurate, very low temperature electron density studies, can provide data of high quality.

Topological analysis of the experimental electron density was carried out and was complemented by theoretical calculations using both *ab initio* CAS-SCF and density functional methods. Somewhat surprisingly, it proved impossible to locate all expected Co−C(alkyne) interactions in the experimental density. Closer analysis of these interactions shows that the electron density in the CoC_2 triangles is very flat, and the theoretical data suggest that the density at the ring and bond critical points differs by less than 0.05 e $Å^{-3}$. In contrast, the residual density of the multipole model is ∼0.1 e $Å^{-3}$ in the vicinity of the transition metal atoms, despite the excellent refinement statistics. We conclude that these errors are so large that they prevent consistent location of all expected critical points in regions of such very flat electron density. Indeed, the atomic arrangement in the CoC_2 part of the molecule is close to being an unstable, so-called catastrophe situation in the QTAIM theory. Compounds of this type represent excellent test cases for experimental electron density modeling.

Neither theory nor experiment finds evidence for a critical point corresponding to a direct Co−Co bond, which is in contravention with the 18-electron rule but in line with theoretical results that suggest singlet diradical character of this compound. This facet was explored in more detail through the source function and the total energy density.

Acknowledgment. We thank DANSYNC for financial support. We appreciate the synthesis efforts by Ms. Marie Chevallier and the assistance during data collection from Dr. Wolfgang Morgenroth. CAS-SCF calculations were done using computer time allocated by the UK National Service for Computational Chemistry Software. Reviewers are acknowledged for some interesting suggestions.

Supporting Information Available: Plots using the conventional model (total density in CoCC planes, selected plots of ρ along lines, and a residual density map); graphical display of ERD axis definitions; tables of complete topological analysis for both conventional and synchrotron models, integrated source functions at the Co−Co midpoints, atomic charges, and refined κ values; detailed data analysis; and a CIF file for **1**. This material is available free of charge via the Internet at http://pubs.acs.org.

JA076152C